12th IEA Heat Pump Conference 2017

Molecular Simulation of NH_3/Ionic Liquid Mixtures for Absorption Heat Pump Cycles

Abhishek Kabra[a], Tim M. Becker[a], Meng Wang[a]*,
Carlos A. Infante Ferreira[a], Thijs J.H. Vlugt[a]

Process and Energy Department, Delft University of Technology, Leeghwaterstraat 39,
2628CB Delft, The Netherlands

Abstract

Force Field based Monte Carlo (MC) simulations are conducted to predict the performance of an absorption heat pump cycle involving NH_3/ionic liquid (IL) (refrigerant/absorbent) as working pair. To investigate the thermodynamic performance of the cycle, various properties such as the enthalpy of absorption, heat capacity, and solubility of refrigerant in the absorbent are required. As an alternative to experiments, MC simulations are used to predict the required properties. The simulations are performed at temperatures ranging from 303 K to 373 K and pressures ranging from 4 to 16 bar. The thermodynamic performance parameters such as the coefficient of performance, *COP*, and the circulation ratio, *f*, of NH_3 paired with [emim][Tf_2N] are investigated using MC simulations and compared to results obtained from correlated experimental data, showing a reasonable agreement. MC simulations could be used as an inexpensive alternative for preliminary design considerations involving potential working pairs for absorption heat pump cycles in the absence of available experimental data.

Selection and/or peer-review under responsibility of the organizers of the 12th IEA Heat Pump Conference 2017.

Keywords: Working pair; Absorption cycle; Monte Carlo simulations; Heat pump; Ionic liquids; NH_3

* Corresponding author. Tel.: +31-617-609-108.
E-mail address: M.Wang-2@tudelft.nl.

Nomenclature

COP	Coefficient of performance	-	mix	Mixing
C	Specific heat	$kJkg^{-1}K^{-1}$	*P*	Constant pressure
f	Circulation ratio	-	r	Refrigerant
h	Enthalpy	$kJkg^{-1}$	s	Weak solution
$\dot{m}$	Mass flow	kgs^{-1}	sol	Solution
P	Pressure	Pa		
Q	Heat flow	W	Superscripts	
T	Temperature	K	IL	Ionic liquid
x	Molar concentration	$molmol^{-1}$	$\overline{n}$	Molar basis
w	Mass concentration	$kg_{IL}kg_{sol}^{-1}$	res	Residual
W_p	Pumping power	W		
			Abbreviations	
Subscripts			EOS	Equation of state
0	Reference state		EXP	Expansion valve
A	Absorber, weak		HX	Heat exchanger
abs	Absorption		IL	Ionic liquid
C	Condenser		MC	Monte Carlo
E	Evaporator		NPT	Isobaric-isothermal ensemble
G	Generator, strong		NRTL	Nonrandom two liquid
IL	Ionic liquid		QM	Quantum mechanical
lat	latent		RK	Redlich-Kwong
			VLE	Vapor-liquid equilibrium

1. Introduction

According to the International Energy Agency (2014) [1], the total energy demand for applications such as space heating and cooling, drying, food storage, etc., is of the order of exajoule (1 EJ = 10^{18} J). To deal with the rapid growth of energy demand and utilization, much attention has been focused on absorption cycles. The advantage of absorption cycles is their effective utilization of low-grade waste heat and the resulting decrease of primary energy consumption [2]. Additionally, heat from renewable sources, such as solar, can be applied as the driving heat. The thermodynamic performance of an absorption cycle depends on its working pair. The commonly used working pairs such as H_2O/LiBr and H_2O/NH_3 are characterized by some drawbacks. These drawbacks are crystallization and low (sub-atmospheric) operating pressure for H_2O/LiBr and a difficult separation (rectification process) for H_2O/NH_3 [3]. ILs have been proposed as alternative absorbents [3-4]. ILs are molten salts which are often liquid at room temperature. They consist of an organic cation and an organic or inorganic anion. ILs are promising absorbents due to their favourable properties such as negligible vapour pressure, high thermal and chemical stability, non-flammability, low corrosive character, and excellent solvation properties [4-5]. Furthermore, billions of ILs with diverse properties can be designed and synthesized by combining different anions and cations. To investigate the thermodynamic performance of an absorption heat pump cycle, various properties such as the enthalpy of absorption, heat capacity, and solubility of refrigerant in the absorbent are required at different state points in the cycle. However, for ILs there are only limited experimental data available. MC simulations and quantum mechanical (QM) calculations can be used to compute the required properties [6]. The accuracy of results from these simulations for predicting the thermodynamic performance for IL/NH_3 heat pump cycles is still unknown. The objective is to apply MC simulation techniques along with QM calculations to determine the thermodynamic properties of working pairs

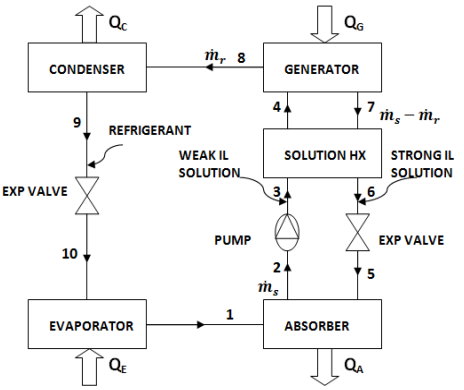

Fig. 1. Schematic representation of a single-effect absorption heat pump cycle.

to investigate their thermodynamic performance in a single-effect absorption heat pump cycle. In this work, NH_3 (refrigerant) is paired with [emim][Tf_2N] (absorbents). [emim][Tf_2N] is selected because it is one of the most widely investigated ILs [3, 7-9].

2. The Absorption Heat Pump Cycle

2.1 Cycle description and thermodynamic model

Fig. 1 shows a schematic representation of the single-effect absorption heat pump cycle using a NH_3/IL mixture as working pair. For a detailed description of the single-effect heat pump cycle we refer to Wang & Infante Ferreira [10]. To simulate the thermodynamic performance of the single-effect absorption heat pump cycle, the following assumptions are made to simplify the calculations:

1. The flow through the components is under steady state.
2. The pressure drop due to friction in the connecting pipelines is neglected. Therefore, the operating pressures in the condenser and the generator are equal (P_C=P_G). Similarly, the operating pressures in the evaporator and the absorber are equal (P_E=P_A).
3. The refrigerant leaves the evaporator (state point 1) as saturated vapour at the dew point with T=T_E=T_1 and the condenser (state point 9) as saturated liquid at the bubble point with T=T_C=T_9.
4. The solution leaves the generator in equilibrium as saturated liquid at its end generation temperature, i.e., T_7=T_G.
5. The refrigerant enters the condenser (state point 8) as superheated vapour at the temperature which is equal to the end generation temperature, i.e., T_8=T_G.
6. The condition at state 2 (solution outlet of the absorber) is a subcooled weak IL solution with a degree of subcooling set to 5 K.
7. The minimal heat transfer temperature difference of the solution HX is set to 5 K.
8. The heat loss through connecting pipes and solution heat exchanger is negligible.

2.2 Cycle performance

Two important parameters for evaluating the thermodynamic performance of a single-effect absorption heat pump cycle are the circulation ratio, *f* and the coefficient of performance, *COP*. The circulation ratio, *f,* is defined as

$$f = \frac{\dot{m}_S}{\dot{m}_r} = \frac{w_G}{w_G - w_A} \quad (1)$$

where w_G and w_A are the mass fractions of the absorbent in the strong and weak IL solutions flowing out of the generator (G) and absorber (A), respectively. $\dot{m}_s$ is the mass flow rate of the weak IL solution flowing out of the absorber and $\dot{m}_r$ is the mass flow rate of the refrigerant (NH_3). In Eq. (1), w_G and w_A are obtained from solubility data. The coefficient of performance, *COP*, of a single-effect heat pump cycle is defined as

$$COP = \frac{Q_C + Q_A}{Q_G + W_P} = \frac{Q_E}{Q_G + W_P} + 1 \tag{2}$$

where Q_C, Q_A, Q_G, and W_P are the heats exchanged with the surrounding and the pumping work. For an NH_3/IL mixture, the enthalpy of the solution, h_{sol} is expressed as

$$h_{sol} = w_{NH_3} h_{NH_3} + w_{IL} h_{IL} + h_{abs} \tag{3}$$

in which h_{NH_3} and h_{IL} are the enthalpy of pure NH_3 and IL at the investigated state, w_{NH_3} and w_{IL} are the mass fractions of NH_3 and IL, respectively, and h_{abs} is the enthalpy of absorption. The enthalpy of pure IL can be obtained as follows

$$h_{IL} = h_0 + \int_{T_0}^{T} C_P^{IL} dT \tag{4}$$

in which h_0 is the reference enthalpy at T_0 and P_0 and C_P^{IL} is the heat capacity of the pure IL. The conditions T_0 = 250.15 K and P_0 = 1 MPa are adopted as an arbitrary reference state for Eq. (4).

3. Property predictions

The above cycle description illustrates that three properties are essential for the performance assessment of absorption heat pump cycles. These properties are the solubility of the absorbent in the refrigerant, the heat capacity of the pure components, and the enthalpy of absorption of the refrigerant/absorbent mixture. MC simulations in the osmotic ensemble are performed to compute the solubility of NH_3 in IL [11-14]. The heat capacity can be divided in an ideal and a residual part. The ideal gas part of the heat capacity of pure IL is computed using QM calculations. The residual part of the heat capacity is computed using MC simulations in the isobaric – isothermal (NPT) ensemble. The enthalpy of absorption for the mixture is calculated using MC simulations in the osmotic ensemble and in the NPT ensemble. For details on the conducted simulations and the applied force fields we refer to Becker et al. [15].

4. Results and discussions

4. 1 Solubility of NH_3 in [emim][Tf_2N]

The solubility of NH_3 in [emim][Tf_2N] is computed at 308.15 and 373.15 K and for pressures between 4 bar and 16 bar. The results are shown in Fig. 2. The experimental data are taken from literature [7-8]. The experimental data are fitted (correlated) with the NRTL model. Details on the NRTL model and the correlated parameters can be found in literature [16]. The results from MC simulations are in reasonable quantitative agreement with the correlated experimental data. The results indicate high solubilities of NH_3 in [emim][Tf_2N]. Simulations yield a solubility trend that is qualitatively similar to that observed in the correlated data. The solubility increases with increasing pressure at constant temperature, and decreases with increasing temperature at constant pressure. The MC simulations overestimate the solubility of NH_3 in [emim][Tf_2N]. Quantitative deviations in the solubilities may be attributed to the applied force fields. For higher accuracy, improvements in the force fields are desired.

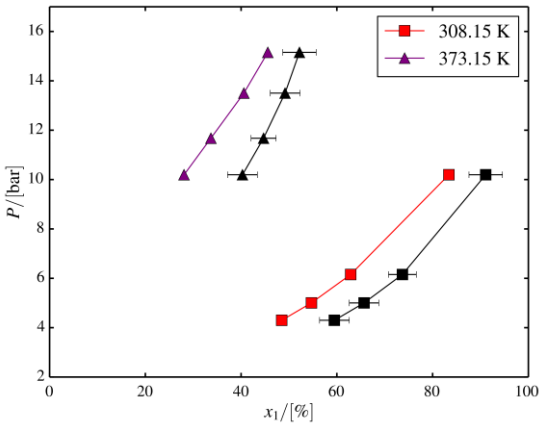

Fig.2. Computed (coloured) and NRTL correlated (black) solubilities of NH_3 (x_1) in [emim][Tf_2N].

4.2 Heat Capacity of ILs

Fig. 3 shows the comparison between the computed and the experimental heat capacities as a function of temperature. The computed results are in good agreement with the experimental data. It is worth noting that the statistical uncertainties of the computed heat capacities are large. However, the uncertainties associated with the experiments are comparable. Consequently, the different experimental data sets for [emim][Tf_2N] show a high degree of scatter.

The computed heat capacities are fitted to a quadratic polynomial in temperature. The fitted parameters are listed in Table 1.

Table 1. Fitted parameters of the computed heat capacity $\bar{C}_P^{\mathrm{IL}} = a + bT + cT^2$ for [emim][Tf2N].

ILs	*a*/ [J mol^{-1} K^{-1}]	*b*/ [J mol^{-1} K^{-2}]	*c*/ [J mol^{-1} K^{-3}]
[emim][Tf2N]	-168.07	2.8714	-2.5159 x 10-3

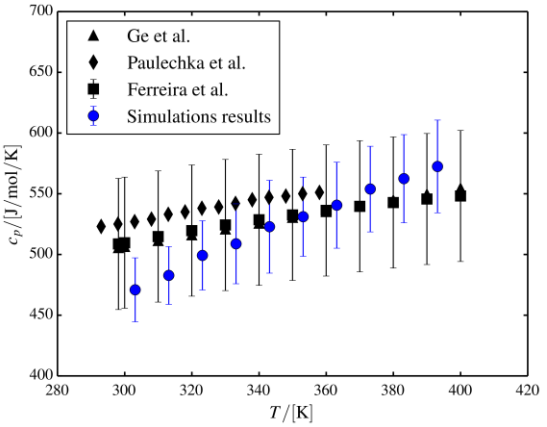

Fig. 3. Comparison of the computed heat capacities (blue symbols) with the experimental heat capacities (black symbols) for [emim][Tf_2N]. Experimental data are taken from Refs. [17-19].

The enthalpies of the pure IL at different conditions are then calculated using Eq. (4). Subsequently, the enthalpies can be used to calculate the *COP* of the absorption heat pump cycle (Eq. (2)). For *COP* calculations from experimental data, experimental heat capacities are fitted to a polynomial. The fitted parameters are taken from literature [16]. The enthalpies of pure NH_3 are obtained from NIST's Refprop [20].

4.3 Enthalpy of absorption

Besides MC simulations, the mixing enthalpy, $\bar{h}_{\mathrm{mix}}$ is frequently derived from the residual enthalpies using a cubic equation of state (EOS). For example, the generic Redlich-Kwong (RK) EOS can be used in combination with a mixing rule based on the experimental vapour-liquid equilibrium (VLE) data.

$$\bar{h}_{\mathrm{mix}} = -x_{\mathrm{NH_3}}\bar{h}^{\mathrm{res}}_{\mathrm{NH_3}} - x_{\mathrm{IL}}\bar{h}^{\mathrm{res}}_{\mathrm{IL}} + \bar{h}^{\mathrm{res}}_{\mathrm{sol}} \tag{5}$$

The detailed procedure and the used parameters are given by Yokozeki & Shiflett [7-8]. The enthalpy of absorption, Δh_{abs} can be determined from the mixing enthalpy by subtracting the latent heat Δh_{lat} (here taken from NIST Refprop [20]).

$$\Delta h_{\mathrm{abs}} = \Delta h_{\mathrm{mix}} - w_{\mathrm{NH_3}}|\Delta h_{\mathrm{lat}}| \tag{6}$$

For comparison, the enthalpies of absorption computed from RK-EOS and from MC simulations are reported in Table 2.

Table 2. Enthalpies of absorption for NH_3/[emim][Tf_2N] computed from MC simulations and RK-EOS.

ILs	*T*/ [K]	*P*/ [bar]	MC Simulation results			RK-EOS results	
			$\Delta\bar{h}_{\mathrm{abs}}$ / [kJ mol^{-1}]	$w_{\mathrm{NH_3}}$ / [kg kg^{-1}]	Δh_{abs} / [kJ kg^{-1}]	$w_{\mathrm{NH_3}}$ / [kg kg^{-1}]	h_{abs} [a] / [kJ kg^{-1}]
[emim][Tf2N]	308.15	6.15	-16.7±1.3	0.1086	-144.2	0.0688	-69.97
	313.15	13.5	-15.0±0.8	0.0404	-72.4	0.0290	-28.0
	373.15	13.5	-10.7±0.9	0.0404	-51.5	0.0290	-22.60

[a]: Enthalpies of absorption computed from RK-EOS using Eqs. (5) and (6).

The enthalpies of absorption computed from MC simulations and from RK-EOS are negative in all cases and show a consistent behaviour. The magnitude of the enthalpy of absorption from MC simulations increases as the temperature decreases. This is in agreement with the results reported by Shi & Maginn [9]. In contrast to the MC simulations, the RK-EOS predicts a smaller temperature dependency of the enthalpy of absorption. Due to a lack of experimental measurements it is difficult to draw any conclusion about the quality of both approaches. However, approaches based on EOS are known to have difficulties in handling the phase behaviour of polar compounds like ILs [21]. Furthermore, the EOS based approach is sensitive to the parameters obtained by fitting to experimental data. Accurate predictions of the enthalpy of absorption seem to be challenging and further investigations are required.

4.4 Circulation ratio, f

The solubility from MC simulations are used to calculate *f*. Subsequently, *f* is compared with the value calculated from the correlated experimental data. Table 3 shows the comparison for an end generation temperature of 100 °C. Large deviations between *f* calculated from these two approaches can be observed. These deviations result from the differences in the predicted solubilities of NH_3. The MC simulations overestimate the solubility of NH_3 which results in low mass fractions of IL. Therefore, the value of *f* is lower. A high circulation ratio increases the pumping power and the generator heat input requirements. Hence, a lower

COP value will be achieved.

Table 3. Comparison of the circulation ratio, f , and coefficient of performance, *COP,* computed from correlated experimental data and simulations. Cycle conditions: T_C = 35 ºC, T_A = 30 ºC, T_E = 10 ºC, T_G =*100* ºC, P_E = 6.15 bar and P_C = 13.5 bar.

Working pair	Method	T_G / [ºC]	w_G / [kgkg^{-1}]	w_A / [kgkg^{-1}]	f	f^a	*COP*	*COP*^{a}
[emim][Tf2N]	correlated data	100	0.971	0.931	24.3	------	1.68	------
	simulations	100	0.959	0.891	14.1	10.8-19.2	1.66	1.63-1.69

f^a and *COP*^{a} are circulation ratio and the coefficient of performance ranges due to uncertainty in the simulation results.

4.5 *Coefficient of performance, COP*

Table 3 also shows the *COP* calculated from correlated experimental data and MC simulations for an end generation temperature of 100 ºC. The approaches agree reasonably well. A smaller value of f is obtained from MC simulations. This is compensated by a larger enthalpy difference between solutions entering (state point 4) and leaving (state point 7) the generator predicted from MC simulations. This enthalpy difference is mainly due to the deviations in the enthalpies of absorption as the deviations in the heat capacities are not significant. The larger enthalpy difference results in a larger generator heat input value. Since the evaporation heat is constant (for a fixed T_E)., the larger generator heat input decreases the *COP* according to Eq. (2).

5. Conclusions

MC simulations and QM calculations have been used to predict all essential properties to assess the performance of the absorption heat pump cycle for the NH_3/IL working pair. To estimate the accuracy of simulations in predicting the thermodynamic performance, the *COP* and the value of f of NH_3/[emim][Tf_2N] are calculated. The results are compared with those obtained using correlated experimental data (NRTL & RK-EOS). MC simulations have been shown to be capable of making qualitative as well as reasonable quantitative predictions of the thermodynamic properties such as heat capacity, solubility and enthalpy of absorption. Therefore, MC simulations have potential to be used to extend the range of the experimental data. Improved force fields that describe the interactions better will yield in better estimates. Hence, this approach can be used as an inexpensive alternative for preliminary design considerations involving potential working fluids for absorption heat pump cycles. Especially, in the absence of experimental data this seems to be the best available approach.

Acknowledgement

This work was sponsored by NWO Exacte Wetenschappen (Physical Sciences) for the use of supercomputer facilities, with financial support from the Nederlandse Organisatie voor Wetenschappelijk Onderzoek (Netherlands Organization for Scientific Research, NWO). TJHV would like to thank for financial support from NWO-CW (Chemical Sciences) for a VICI grant. MW and CAIF acknowledge support from the China Scholarship Council for this research.

References

[1] IEA. World Energy Outlook. International Energy Agency (IEA); 2014.

[2] Wasserscheid P, Seiler M. Leveraging Gigawatt Potentials by Smart Heat-Pump Technologies Using Ionic Liquids. *Chem. Sus. Chem*; 2011; **4**; 459-463.

[3] Zheng D, Dong L, Huang W, Wu X, Nie N. A review of imidazolium ionic liquids research and development towards working pair of absorption cycle. *Renew. Sustain. Energy Rev*; 2014; **37**; 47–68.

[4] Yokozeki A. Theoretical performances of various refrigerant – absorbent pairs in a vapor-absorption refrigeration cycle by the use of equations of state. *Appl. Energy*; 2005; **80**; 383–399.

[5] Ramdin M, de Loos TW, Vlugt TJH. State-of-the-art of CO_2 capture with ionic liquids. *Indus. Eng. Chem. Research*; 2012; **51**; 8149-8177.
[6] Liu H., Maginn EJ., Visser AE., Bridges NJ., Fox EB. Thermal and Transport Properties of Six Ionic Liquids: An Experimental and Molecular Dynamics Study. Ind. Eng. Chem. Res;2012; 51:7242–7254.
[7] Yokozeki A, Shiflett MB. Ammonia Solubilities in Room-Temperature Ionic Liquids. *Ind. Eng. Chem. Res*; 2007a; **46**; 1605–1610.
[8] Yokozeki A, Shiflett MB. Vapor-liquid equilibria of ammonia + ionic liquid mixtures. *Appl. Energy*; 2007b; **84**; 1258–1273.
[9] Shi W, Maginn EJ. Molecular Simulation of Ammonia Absorption in the Ionic Liquid 1-ethyl-3- methylimidazolium bis (trifluoromethylsulfonyl)imide ([emim][Tf2N]). *AIChE J*; 2009; **55**; 405–410.
[10] Wang M, Infante Ferreira CA. Absorption Heat Pump Cycles with NH_3 – Ionic Liquid Working Pairs. in review
[11] Ramdin M, de Loos TW, Vlugt TJH, Balaji SP, Calero S, Sevillano JJG, Luna JMV. Solubility of the precombustion gases CO_2, CH_4, CO, H_2, N_2, and H_2S in the ionic liquid [bmim][Tf_2N] from Monte Carlo Simulations. *J. Phys. Chem. C*; 2014; **118**; 23599-23604.
[12] Ramdin M, Chen Q, Vlugt TJH, Balaji SP, Bardow A, Sevillano JJG, Goetheer E. Validation of the CO_2/N_2O analogy using Molecular Simulation. *Indus. & Eng.Chem. Research*; 2014; **46**; 18081-18090.
[13] Ramdin M, de Loos TW, Vlugt TJH, Balaji SP, Calero S, Luna JMV, Knoop AT, Chen Q, Dubbeldam D. Computing bubble points of CO_2/CH_4 gas mixtures in ionic liquids from Monte Carlo Simulations. *Fluid Phase Equilib.*; 2016; **418**; 100-107.
[14] Ramdin M, de Loos TW, Vlugt TJH, Balaji SP, Calero S, Luna JMV, Knoop AT, Chen Q, Dubbeldam D. Solubility of CO_2, CH_4, C_2H_6, and SO_2 in ionic liquids and Selexol from Monte Carlo Simulations. *J. Comp. Sci.*; 2015.
[15] Becker TM, Wang M, Kabra A, Jamali SH, Ramdin M, Dubbeldam D, Infante Ferreira CA, Vlugt TJH. Computational Performance Prediction of Absorption Refrigeration Cycles with Ammonia – Ionic Liquid Working Pairs. in preparation
[16] Wang M, Infante Ferreira CA. Performance Prediction of Single-Effect Absorption Heat Pump Cycles using Ionic Liquids. Proceedings of the 12th IIR Gustav Lorentzen Natural Working Fluids Conference, 2016.
[17] Ge R, Hardacre C, Jacquemin J, Nancarrow P, Rooney DW. Heat capacity of ionic liquids as a function of temperature at 0.1 MPa. Measurement and prediction. *J. Chem. Eng. Data*; 2008; **53**; 2148-2153.
[18] Paulechka YU, Blokhin AV, Kabo GJ, Strechan AA. Thermodynamic properties and polymorphism of 1-alkyl-3-methylimidazolium bis(triflamides). *J. Chem. Thermodyn.*; 2007; **39**; 866–877.
[19] Ferreira FA, Simões PN, Ferreira AGM. Quaternary phosphonium-based ionic liquids: Thermal stability and heat capacity of the liquid phase. *J. Chem. Thermodyn.*; 2012; **45**; 16–27.
[20] Lemmon EW, Huber ML, McLinden MO. NIST reference fluid thermodynamic and transport property – Refprop. 2013.
[21] Fermeglia M, Kikic I. Excess enthalpy calculations by means of equation of state. *Therm. Anal. J.*;1984;**129**;687-695.